Supporting information

Solution-Processed Bilayered ZnO Electron Transport Layer for Efficient Inverted Non-Fullerene Organic Solar Cells

Walia Binte Tarique[a*], Md Habibur Rahaman[b], Shahriyar Safat Dipta[a], Ashraful Hossain Howlader[a], and Ashraf Uddin[a*]

a School of Photovoltaic and Renewable Energy Engineering, University of New South Wales, Sydney, NSW 2052, Australia

b School of Chemistry, University of New South Wales, Sydney, NSW 2052, Australia

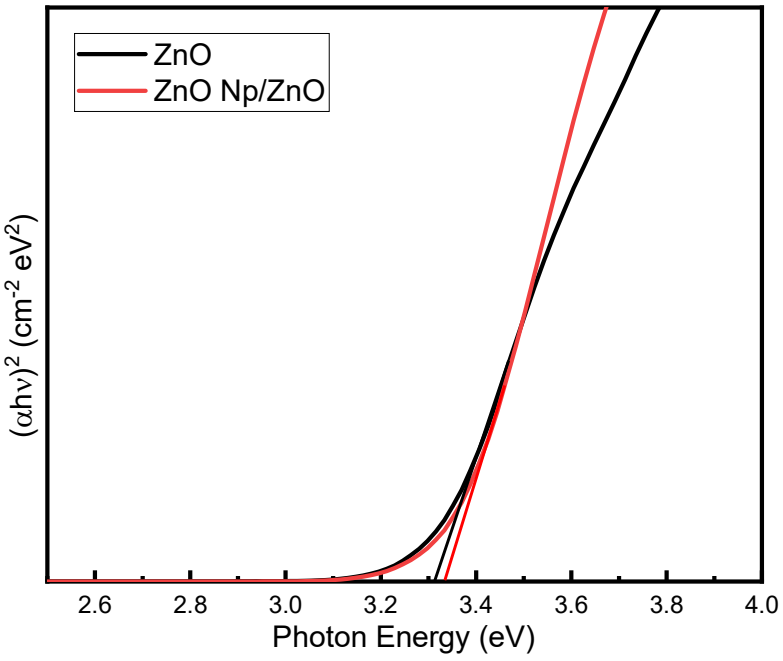

Figure S1. Bandgap of ZnO ETL and ZnO NP/ZnO ETL determined from the Tauc plot.

(a)

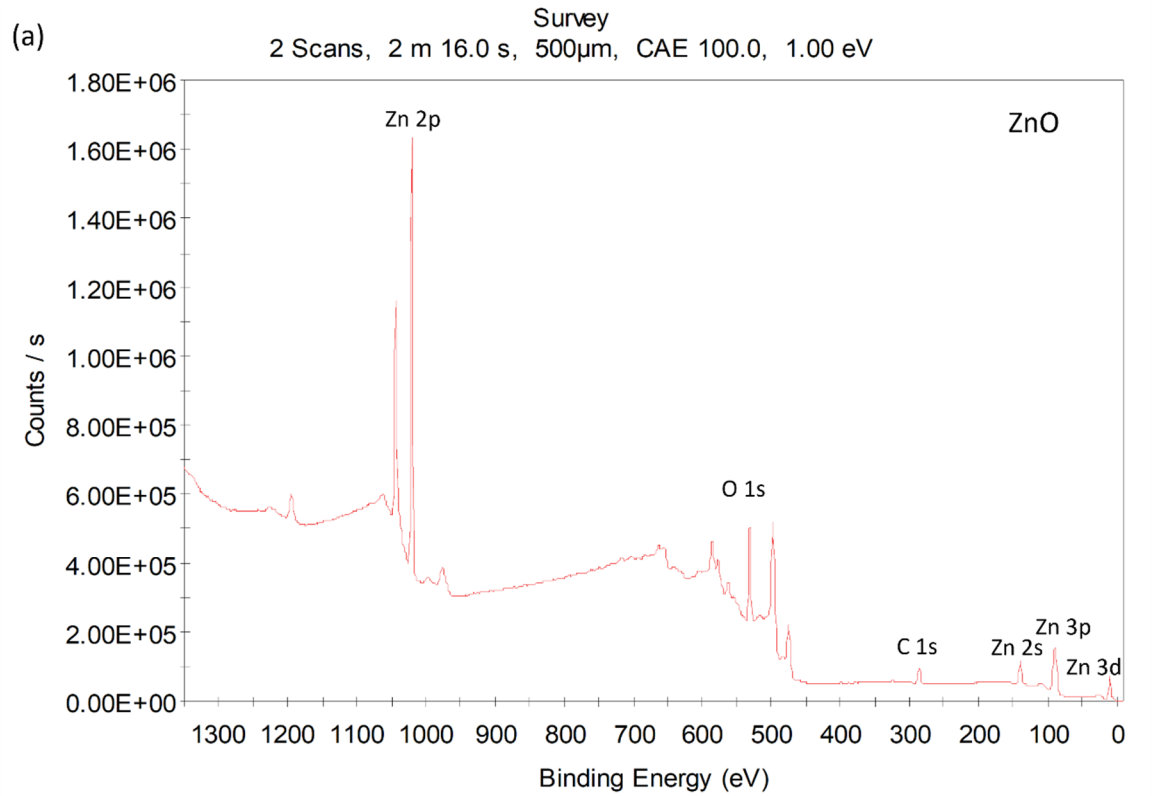
Survey
2 Scans, 2 m 16.0 s, 500µm, CAE 100.0, 1.00 eV
ZnO
Zn 2p
O 1s
C 1s
Zn 2s
Zn 3p
Zn 3d
Counts / s
Binding Energy (eV)
1.80E+06
1.60E+06
1.40E+06
1.20E+06
1.00E+06
8.00E+05
6.00E+05
4.00E+05
2.00E+05
0.00E+00
1300 1200 1100 1000 900 800 700 600 500 400 300 200 100 0

(b)

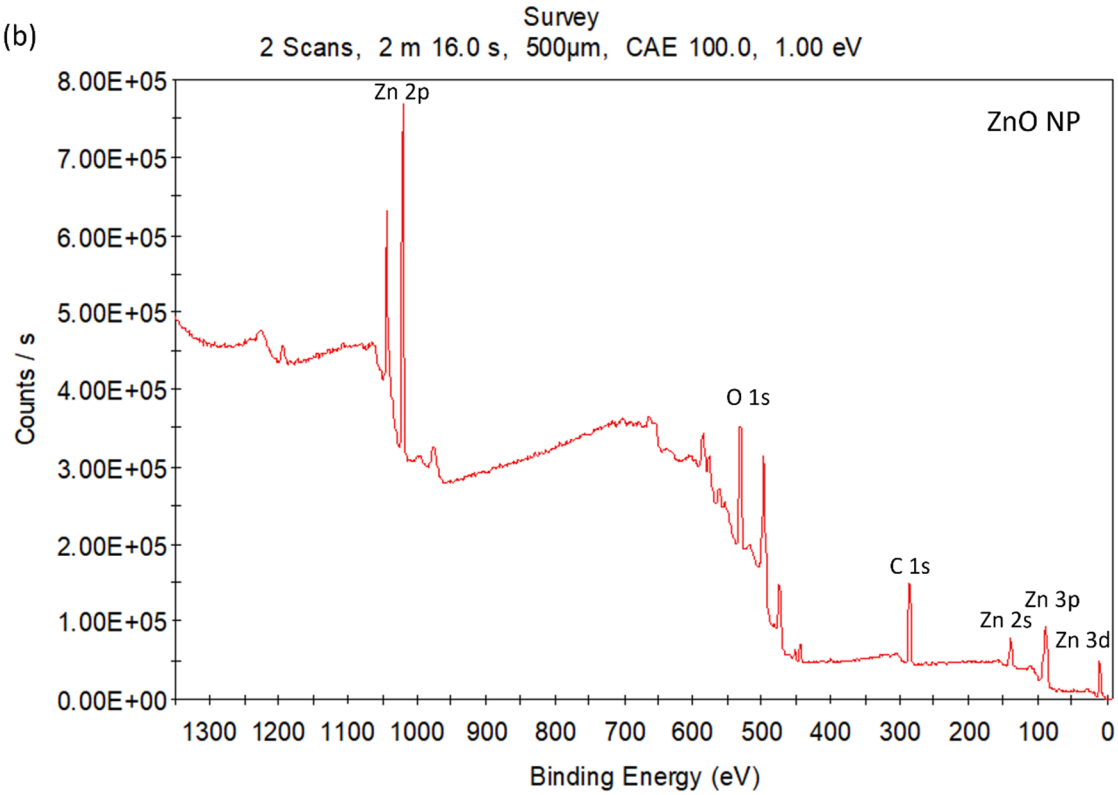
Survey
2 Scans, 2 m 16.0 s, 500µm, CAE 100.0, 1.00 eV
ZnO NP
Zn 2p
O 1s
C 1s
Zn 2s
Zn 3p
Zn 3d
Counts / s
Binding Energy (eV)
8.00E+05
7.00E+05
6.00E+05
5.00E+05
4.00E+05
3.00E+05
2.00E+05
1.00E+05
0.00E+00
1300 1200 1100 1000 900 800 700 600 500 400 300 200 100 0

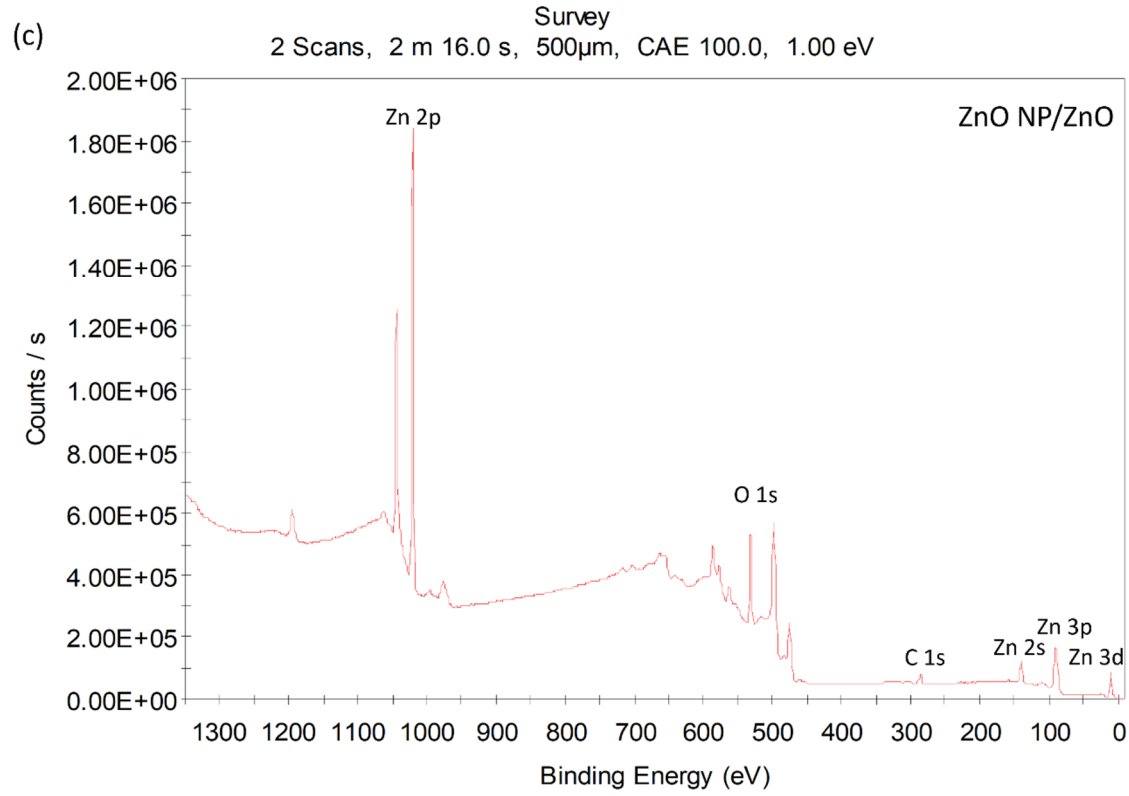

Figure S2. X-Ray photoelectron spectroscopy (XPS) survey spectra of (a) ZnO, (b) ZnO-NP and (c) bilayer ETLs, on ITO/glass substrate, demonstrating the elemental peaks.

Table S1: Photovoltaic parameters of organic solar cells with ZnO-based electron transport layer (ETL)

ELT	Donors	Acceptors	V_{oc} [V]	J_{sc} [mA cm^{-2}]	*FF* [%]	PCE [%]	[Ref]
Li-doped ZnO	PTB7-Th	IT-4F	0.83	16.20	67	8.96	[1]
KOH-ZnO	PBDB-T-2CL	Y1-4F	0.84	23.0	78.3	63	[2]
ZnO/C_{60}-SAM	PTB7-Th	IEICO-4F	0.71	22.70	60	7.40	[3]
ZnO:PFN-Br	PBDB-T	IT-4F	0.87	20.02	79	13.82	[4]
ZnO/TiO2	PTB7-Th	IEICO-4F	0.7	24.2	61.1	10.3	[5]
ZnO/ASP-SWNT	PM6	Y6	0.87	24.90	66	14.37	[6]

CsI/ZnO	PTB7	$PC_{71}BM$	0.73	17.6	56.6	7.3	[7]
MgO/ZnO	PTB7-Th	$PC_{71}BM$	0.80	19.28	71.51	11.01	[8]
In2O3/ZnO (NP)	PTB7-Th	$PC_{71}BM$	0.81	18.3	66	9.8	[9]
ZnO/glycine	PM6	IT-4F	0.85	22.01	75	14	[10]

Table S2: XRD parameters for ZnO, ZnO NP, and ZnO NP/ZnO ELTs.

Sample	Peak position [2θ]	d-spacing [Å]	FWHM [°2θ]	Crystallite Size only [nm]
ZnO	31.7409	2.81683	0.614	13.45
	34.1538	2.62314	1.4327	5.80
	36.1542	2.48246	0.614	13.61
ZnO NP	31.6569	2.82411	0.4093	20.17
	34.262	2.61511	0.7164	11.60
	36.0083	2.49218	0.3582	23.32
ZnO NP/ZnO	31.8081	2.81103	0.4093	20.18
	34.3373	2.60954	0.614	13.54
	36.0687	2.48815	0.307	27.21

Table S3: Peak binding energy, peak full width at half maximum, and atomic percentage of ETL films (ZnO, ZnO-NP and bilayer) from X-Ray photoelectron spectroscopy (XPS) data.

ETL	**Peak**	**Start Binding**	**Peak Binding**	**End Binding**	**Full Width at Half**	**Atomic Percentage**

		Energy (eV)	Energy (eV)	Energy (eV)	Maximum (FWHM) (eV)	(%)
ZnO	O_{1s} A	539.1	529.87	523.1	1.08	14.45
	O_{1s} B	539.1	531.32	523.1	2.22	29.66
ZnO-NP	O_{1s} A	539.1	529.51	523.1	1.31	13.93
	O_{1s} B	539.1	532.35	523.1	1.78	18.11
	O_{1s} C	539.1	530.6	523.1	1.31	8.02
Bilayer	O_{1s} A	539.3	530.11	523.3	1.13	22.01
	O_{1s} B	539.3	531.68	523.3	1.76	23.86

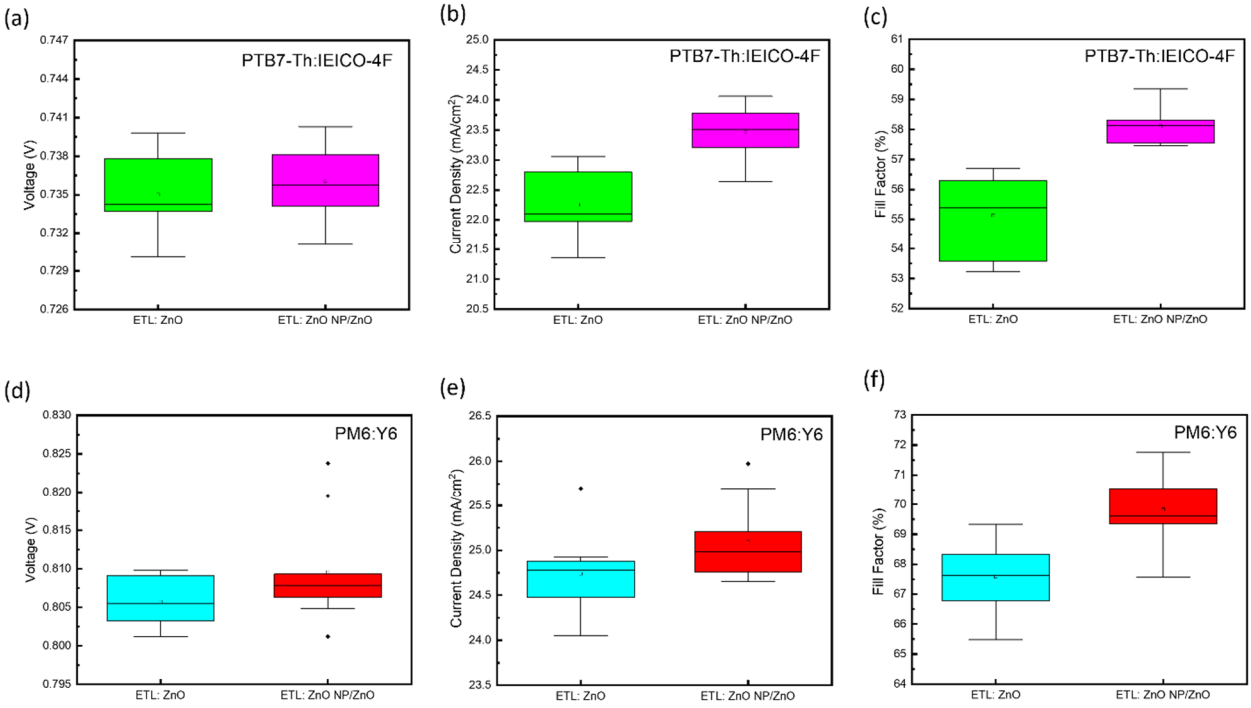

Figure S3. Statistical distribution of the device parameters (devices with ZnO and bilayer ZnO NP/ZnO) displayed (a,d) V_{oc} (V), (b,e) J_{sc} (mA/cm^2), and (c,f) *FF* (%). 10 cells have been tested for each case. A bilayer device exhibits a simultaneous improvement in all photovoltaic parameters compared to the ZnO control device.

Table S4: Electrical parameters extracted from Nyquist plot for ZnO only and ZnO NP/ZnO devices

Device	Parameters	ZnO ETL	ZnO NP/ZnO ETL	Unit
PTB7-Th:IEICO-4F	Series resistance, R_s	152	143	Ω
	Transport resistance, R_t	545	618	Ω
	Recombination resistance, R_{rec}	7.47	10.9	KΩ
	Bulk capacitance, C_g	10.9	9.68	nF
	Chemical capacitance, C_μ	5.89	4.47	nF
PM6:Y6	Series resistance, R_s	82.8	74.5	Ω
	Transport resistance, R_t	848.2	953	Ω
	Recombination resistance, R_{rec}	2.46	6.35	KΩ
	Bulk capacitance, C_g	4.35	6.31	nF
	Chemical capacitance, C_μ	11.2	3.23	nF

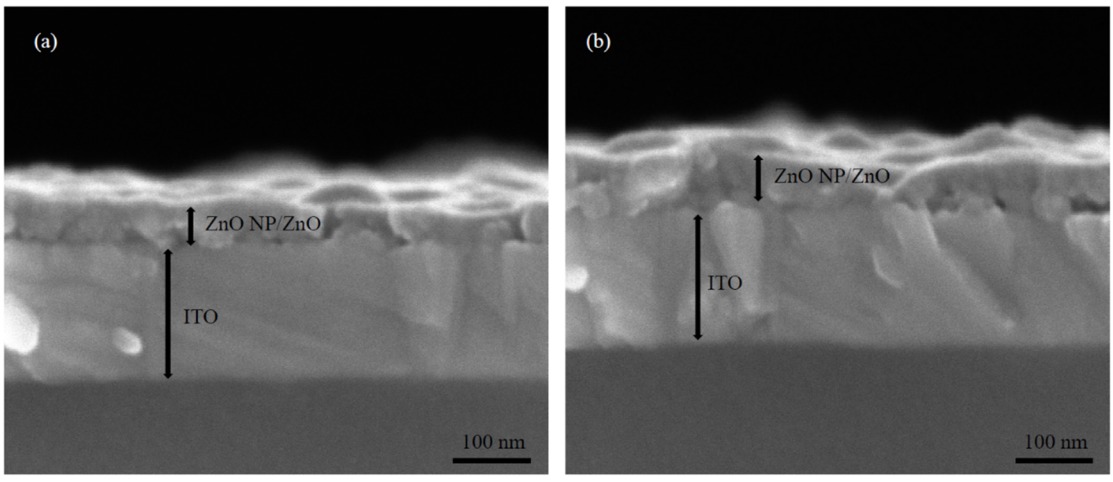

Figure S4. (a,b) Cross-section SEM images of fresh and aged bilayer ZnO NP/ZnO ETL.

References

1. Soultati, A.; Fakharuddin, A.; Polydorou, E.; Drivas, C.; Kaltzoglou, A.; Haider, M.I.; Kournoutas, F.; Fakis, M.; Palilis, L.C.; Kennou, S.; et al. Lithium Doping of ZnO for High Efficiency and Stability Fullerene and Non-Fullerene Organic Solar Cells. *ACS Appl. Energy Mater.* **2019**, *2*, 1663–1675, https://doi:10.1021/acsaem.8b01658.
2. Cheng, H.-W.; Raghunath, P.; Wang, K.; Cheng, P.; Haung, T.; Wu, Q.; Yuan, J.; Lin, Y.-C.; Wang, H.-C.; Zou, Y.; et al. Potassium-Presenting Zinc Oxide Surfaces Induce Vertical Phase Separation in Fullerene-Free Organic Photovoltaics. *Nano Lett.* **2020**, *20*, 715–721, https://doi:10.1021/acs.nanolett.9b04586.
3. Xu, X.; Xiao, J.; Zhang, G.; Wei, L.; Jiao, X.; Yip, H.-L.; Cao, Y. Interface-Enhanced Organic Solar Cells with Extrapolated T80 Lifetimes of over 20 years. *Science Bulletin* **2020**, *65*, 208–216, https://doi:10.1016/j.scib.2019.10.019.
4. Zheng, Z.; Zhang, S.; Wang, J.; Zhang, J.; Zhang, D.; Zhang, Y.; Wei, Z.; Tang, Z.; Hou, J.; Zhou, H. Exquisite Modulation of ZnO Nanoparticle Electron Transporting Layer for High-Performance Fullerene-Free Organic Solar Cell with Inverted Structure. *J. Mater. Chem. A* **2019**, *7*, 3570–3576, https://doi:10.1039/C8TA11624E.
5. Habibur Rahaman, M.; Sang, B.; Anower Hossain, Md.; Hoex, B.; Mota-Santiago, P.; Mitchell, V.D.; Uddin, A.; Stride, J.A. Impact of the Bilayer Electron Transport Layer in the Donor Acceptor Bulk Heterojunctions for Improved Inverted Organic Photovoltaic Performance. *Applied Surface Science* **2023**, *612*, 155669, https://doi:10.1016/j.apsusc.2022.155669.
6. Lee, S.-H.; Ko, S.-J.; Eom, S.H.; Kim, H.; Kim, D.W.; Lee, C.; Yoon, S.C. Composite Interlayer Consisting of Alcohol-Soluble Polyfluorene and Carbon Nanotubes for Efficient Polymer Solar Cells. *ACS Applied Materials & Interfaces* **2020**, https://doi:10.1021/acsami.9b22933.
7. Upama, M.B.; Elumalai, N.K.; Mahmud, M.A.; Wright, M.; Wang, D.; Xu, C.; Haque, F.; Chan, K.H.; Uddin, A. Interfacial Engineering of Electron Transport Layer Using Caesium Iodide for Efficient and Stable Organic Solar Cells. *Applied Surface Science* **2017**, *416*, 834–844, https://doi:10.1016/j.apsusc.2017.04.164.
8. Huang, S.; Kang, B.; Duan, L.; Zhang, D. Highly Efficient Inverted Polymer Solar Cells by Using Solution Processed MgO/ZnO Composite Interfacial Layers. *Journal of Colloid and Interface Science* **2021**, *583*, 178–187, https://doi:10.1016/j.jcis.2020.09.047.
9. Eisner, F.; Seitkhan, A.; Han, Y.; Khim, D.; Yengel, E.; Kirmani, A.R.; Xu, J.; García de

Arquer, F.P.; Sargent, E.H.; Amassian, A.; et al. Solution-Processed In2O3/ZnO Heterojunction Electron Transport Layers for Efficient Organic Bulk Heterojunction and Inorganic Colloidal Quantum-Dot Solar Cells. *Solar RRL* **2018**, *2*, 1800076, https://doi:10.1002/solr.201800076.

10. Zhu, X.; Guo, B.; Fang, J.; Zhai, T.; Wang, Y.; Li, G.; Zhang, J.; Wei, Z.; Duhm, S.; Guo, X.; et al. Surface Modification of ZnO Electron Transport Layers with Glycine for Efficient Inverted Non-Fullerene Polymer Solar Cells. *Organic Electronics* **2019**, *70*, 25–31, https://doi:10.1016/j.orgel.2019.03.039.